12-2010

Opportunistic Routing in Wireless Sensor Networks Powered by Ambient Energy Harvesting

Zhi Ang EU

Hwee-Pink TAN

Singapore Management University, hptan@smu.edu.sg

Winston K. G. SEAH

DOI: https://doi.org/10.1016/j.comnet.2010.05.012

Published in Computer Networks, 2010 December, 54 (17), pp. 2943–2966.
http://dx.doi.org/10.1016/j.comnet.2010.05.012

Opportunistic Routing in Wireless Sensor Networks Powered by Ambient Energy Harvesting

Zhi Ang Eu[*,a], Hwee-Pink Tan[b], Winston K. G. Seah[c]

[a] *NUS Graduate School for Integrative Sciences and Engineering*
National University of Singapore
CeLS, #05-01, 28 Medical Drive, Singapore 117456
[b] *Networking Protocols Department*
Institute for Infocomm Research (I^2R), A^*STAR
1 Fusionopolis Way, #21-01 Connexis, Singapore 138632
[c] *School of Engineering and Computer Science*
Victoria University, PO Box 600, Wellington 6140, New Zealand

Abstract

Energy consumption is an important issue in the design of wireless sensor networks (WSNs) which typically rely on portable energy sources like batteries for power. Recent advances in ambient energy harvesting technologies have made it possible for sensor nodes to be powered by ambient energy entirely without the use of batteries. However, since the energy harvesting process is stochastic, exact sleep-and-wakeup schedules cannot be determined in WSNs *P*owered solely using *A*mbient *E*nergy *H*arvesters (WSN-HEAP). Therefore, many existing WSN routing protocols cannot be used in WSN-HEAP. In this paper, we design an opportunistic routing protocol (EHOR) for multi-hop WSN-HEAP. Unlike traditional opportunistic routing protocols like ExOR or MORE, EHOR takes into account energy constraints because nodes have to shut down to recharge once their energy is depleted. Furthermore, since the rate of charging is dependent on environmental factors, the exact identities of nodes that are awake cannot be determined in advance. Therefore, choosing an optimal forwarder is another challenge in EHOR. We use a regioning approach to achieve this goal. Using extensive simulations incorporating experimental results from the characterization

[*]corresponding author, telephone number: +65-64082319
Email addresses: euzhiang@nus.edu.sg (Zhi Ang Eu), hptan@i2r.a-star.edu.sg (Hwee-Pink Tan), Winston.Seah@ecs.vuw.ac.nz (Winston K. G. Seah)

of different types of energy harvesters, we evaluate EHOR and the results show that EHOR increases goodput and efficiency compared to traditional opportunistic routing protocols and other non-opportunistic routing protocols suited for WSN-HEAP.
Key words: opportunistic routing, wireless sensor networks, energy harvesting

1. Introduction

Current research on wireless sensor networks [1], and more recently wireless multimedia sensor networks [2], have focused on extending network lifetime [3] since they are powered using finite energy sources (e.g., batteries). Such battery-powered sensor networks are inappropriate for some applications due to environmental concerns arising from the risk of battery leakage and physical/environmental constraints may restrict the ability to replace the batteries or the sensor nodes. Recent advances in ambient energy harvesting technologies [4] have made it possible for sensor nodes to rely on energy harvesting devices for power. Commercially available devices developed by Texas Instruments [5], Microstrain [6] and Ambiosystems [7] can harvest useful energy from solar and vibration energy. They have been deployed in testbeds (e.g. [8], [9]) for scenarios where the sink is within direct transmission range and the harvested energy is used to supplement batteries.

Therefore, *W*ireless *S*ensor *N*etworks (WSNs) *P*owered by *A*mbient *E*nergy *H*arvesting (which we refer to as WSN-HEAP in this paper) are more useful and economical in the long-term since (i) ambient energy such as light, vibration, heat and wind are always available from the environment; (ii) they can operate without disruption due to human intervention to change batteries and (iii) they can operate perpetually by using supercapacitors (with virtually unlimited recharge cycles) to store the harvested energy. Hence, WSN-HEAP are useful for applications such as structural health monitoring [10] where sensors embedded into buildings and structures are not easily accessible after deployment, but yet can tap onto ambient energy sources (e.g. light, vibration, heat, RF etc) for

power. In particular, enabling multi-hop capabilities in WSN-HEAP is useful for such applications, where power supplies are not readily available, thus limiting the number of ac-powered sinks that can be deployed. Most of the existing work on WSNs with energy harvesters focused on harvesting energy to supplement battery power while we focus on using the harvested energy as the only energy source. To the best of our knowledge, none of these efforts address issues related to multi-hop routing in WSNs powered solely using energy harvesters.

The energy characteristics of a WSN-HEAP node are different from that of a battery-powered sensor node, as illustrated in Fig. 1. In a battery-powered sensor node, the total energy reduces with time and the sensor node can operate until the energy level reaches an unusable level. In a WSN-HEAP node, energy can be replenished (charging) and accumulated until a certain level before it can be used. However, as the rate of charging is usually much lower than the rate of energy consumption for the sensor nodes, WSN-HEAP nodes are normally awake for a short period of time before it needs to shut down in order to recharge. Moreover, the time taken to charge up the sensor node to a useful level varies due to environmental factors as well as the type and size of the energy harvesters used. These unique characteristics render the direct application of many routing protocols proposed for battery-powered WSNs unsuitable in WSN-HEAP.

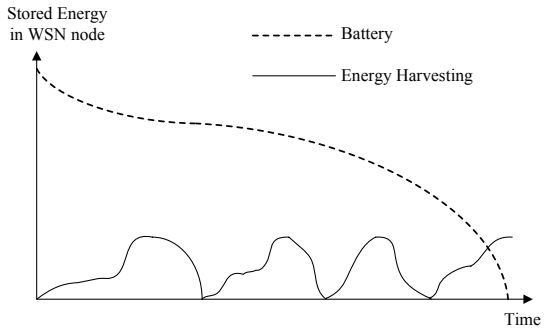

Figure 1: Characteristics of Energy Sources

In this paper, we design an multi-hop energy harvesting opportunistic routing (EHOR) protocol that (i) partitions nodes into regions and (ii) assigns trans-

mission priorities to regions, taking into consideration proximity to the sink and residual energy, so as to minimize collisions while ensuring packet advancement in a multi-hop WSN-HEAP. Using extensive simulations, we demonstrate that EHOR achieves good performance and outperforms traditional opportunistic routing protocols as well as other (non-opportunistic) routing protocols that are applicable to WSN-HEAP. EHOR reduces the cost of deploying WSN-HEAP by extending the range and coverage using multi-hop communications.

The rest of this paper is organized as follows: In Section 2, we review some work on energy harvesting technologies and their application in sensor networks as well as various variants of opportunistic routing protocols used in wireless networks. Then, we present the components of a WSN-HEAP node and characterize the energy and radio characteristics of the nodes in Section 3. Next, we present our opportunistic routing protocol designed for WSN-HEAP in Section 4. The performance results and comparison of EHOR and other routing protocols are presented in Section 5. We conclude the paper in Section 6.

2. Related Work

There are a number of routing protocols designed for use in WSNs with energy harvesting devices. For example, in [11], directed diffusion is modified to incorporate information on whether a node is running on solar power or on battery power. Results show that solar-aware directed diffusion performs better than shortest-path routing. In [12] and [13], a solar-cell energy model is incorporated into geographic routing to improve network performance. Since nodes may harvest different amounts of energy, their duty cycles may not be the same. To reduce latency, a low-latency routing algorithm is proposed in [14]. In WSNs with energy harvesting devices, maximizing the network's goodput is the main consideration since energy can be replenished. However, the amount of power provided by the environment is limited, therefore we need to have a routing algorithm that takes into consideration actual environmental conditions. A solution to this problem is given in [15] and this work is further extended in

[16]. The main idea is to model the network as a flow network and obtain the solution by solving the maxflow problem to maximize throughput. Another solution is given in [17] where the energy replenishment rate is incorporated into the cost metric when computing routes. If batteries are used in conjunction with supercapacitors, then a routing metric can be derived [18] to maximize network life by minimizing the use of the battery since it has limited recharge cycles and maximizing the use of the supercapacitor since it can be recharged millions of times. However, these routing protocols typically require the use of stable links to work well. They do not take advantage of the use of the broadcast nature of the wireless medium as packets are usually addressed to a specific node. Furthermore, some of these routing protocols assume scenarios where energy harvesting is the secondary energy source for the battery which is the primary energy source while in our scenario, the harvested energy is the *only* energy source.

Conventional WSN routing protocols cannot be used in WSN-HEAP since the wakeup timings of the sensor nodes cannot be predicted in advance because the time required to charge up the sensor node fully is dependent on environmental factors. Therefore, it is not possible for a node to know the number or the identity of neighbors who are in receive state when it is ready to transmit. However, assuming that each node knows its own location, we can use a broadcast-based geographic routing protocol to compare with EHOR. In our earlier work [19], we showed that *G*eographic *R*outing with *D*uplicate *D*etection (GR-DD) performs better than geographic routing alone in WSN-HEAP. The flowchart for GR-DD is illustrated in Fig. 2.

Another routing protocol that can be used in WSN-HEAP is unicast routing, where time is slotted and each node wakes up asynchronously according to a Wakeup Schedule Function (WSF) [20]. With a (u, w, v) block design, each node is awake over a block of u slots, and is active over w slots such that any two nodes would have at least v overlapping active slots. In WSN-HEAP, the node will harvest enough energy in each charging cycle to be active in w slots. After charging to the required level, the node will start a new block at the start

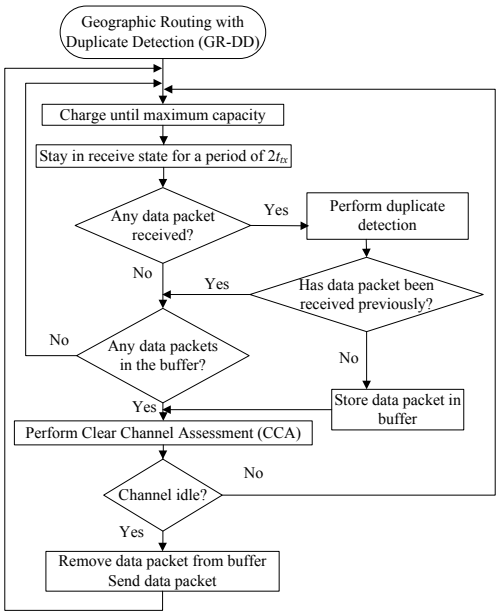

Figure 2: Flowchart for GR-DD Routing Protocol

of the next time slot. If no charging is required within blocks (since the node may accumulate enough energy for the block during the sleep periods within the block), then any two blocks would have at least v active slots in common. The WSF scheme in WSN-HEAP is illustrated in Fig. 3 using a (7,3,1) block design.

In each active slot, the node can either choose to be a receiver or a sender. If it chooses to be a receiver, then it would need to transmit a beacon at the start of the slot to let other senders know that it is ready to receive data. If it chooses to be a sender, it would wait to receive beacons from the receivers. Once a beacon is received successfully by the sender, it would determine whether the sender of the beacon is closer to the sink than it is to determine whether it could be a forwarder. If it could be a forwarder for the sender, the sender will send its data to the receiver. If the receiver receives the data successfully, it would send an acknowledgment packet (ACK) back to the sender.

*O*pportunistic *R*outing (OR) is a scheme that takes advantage of the broad-

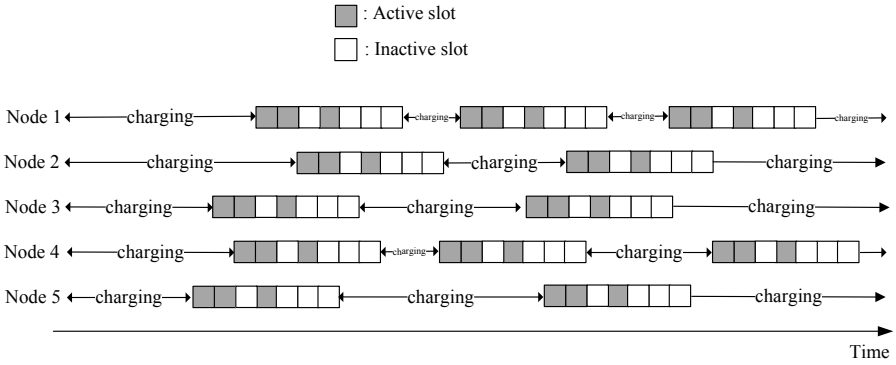

Figure 3: Possible wakeup schedules for different nodes with WSF(7,3,1)

cast nature of the wireless medium to improve link reliability and system throughput in a multi-hop wireless network. It comprises (i) *forwarding candidate selection*, which determines the set of forwarding nodes and (ii) *relay priority assignment*, which determines the transmission priority among the set of forwarding candidates. We illustrate OR using the scenario in Fig. 4 where there is a sender, seven nodes labeled from 1 to 7 and a sink. In the forwarding candidates selection phase, nodes 1 and 2 will drop the received broadcast packet from the sender since they are further away from the sink than the sender is. Since nodes 3 to 7 are closer to the sink than the sender is, they are designated as potential relay nodes for the sender. Next, we need to assign the transmission priorities for relay nodes 3 to 7. Due to shadowing and fading effects, there is a probability that the relay nodes and the sink will receive the broadcast packet from the sender. However, this probability generally decreases with distance. Ideally, if the sink receives the data packet directly from the sender, all the relay nodes should not rebroadcast the received packet. Otherwise, the relay node which is closest to the sink that receives the data packet should forward the received data packet. For example, if nodes 3, 5, and 6 receive the broadcast data packet correctly, only node 6 should forward the data packet.

ExOR [21], MORE [22] and the OpRENU scheme [23] are opportunistic protocols designed based on this concept. However, the performance of these

Figure 4: Example in Opportunistic Routing

protocols is not optimized when used in WSN-HEAP as compared to battery-operated WSNs. This is because WSN-HEAP nodes are not awake at all times since our energy model based on energy harvesters is different from that of a battery-operated sensor node. Furthermore, MORE uses network coding which may not be suitable for resource-constrained WSNs. GeRaF [24] is another protocol that uses RTS/CTS-based receiver contention scheme to select the best forwarders but it uses preceding control packets to determine channel conditions which is not suitable for rapidly changing channel conditions.

3. System Model

3.1. Components of a WSN-HEAP node

Each WSN-HEAP node comprises of various components as illustrated in Fig. 5. The energy harvesting device converts ambient energy into electrical energy. Since the rate of energy harvesting could be significantly lower than the typical power consumption levels in the sensor nodes, the harvested energy is cumulatively stored in an energy buffer. Once the stored energy reaches a useful level, the node will be operable. During the charging phase, the node is idle.

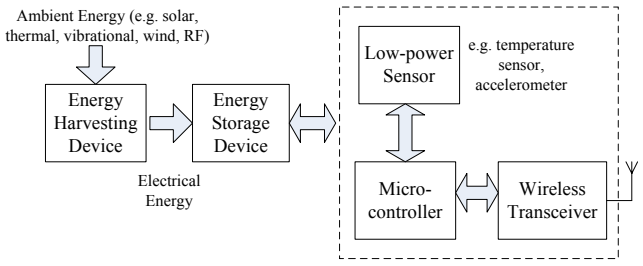

Figure 5: Components of a WSN-HEAP node

3.2. Characterization of WSN-HEAP

In this paper, our main focus is to develop and evaluate multi-hop routing protocols for WSN-HEAP. For an accurate evaluation, we first need to define a realistic model for WSN-HEAP. We do so by empirically characterizing the (i) radio behavior as well as (ii) traffic and energy harvesting characteristics of solar [5] and thermal [25] energy harvesting nodes that use the MSP430 microcontroller and CC2500 radio transceiver from Texas Instruments (TI), as shown in Fig. 6.

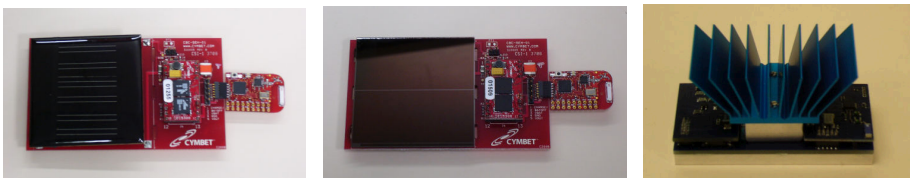

(a) Outdoor Solar Energy Harvester (b) Indoor Solar Energy Harvester (c) Thermal Energy Harvester

Figure 6: Energy harvesting sensor nodes using MSP430 microcontroller and CC2500 transceiver from Texas Instruments

The sensor node development kit [5] we use consists of a solar panel optimized for indoor use, two eZ430-RF2500T target boards and one AAA battery pack. The target board comprises the TI MSP430 microcontroller, CC2500 radio transceiver and an on-board antenna. The CC2500 radio transceiver operates in the 2.4GHz band with data rate of 250Kbps and is designed for low power wireless applications. The harvested energy is stored in EnerChip, a thin-film rechargeable energy storage device with low self-discharge manufactured by Cymbet.

The experimental setup comprises one or more transmitters (with transmission power fixed at 1dBm) and a receiver (sink) connected to a laptop as shown in Fig. 7a and 7b. The battery pack is used for powering the target board at the transmitter in the radio characterization tests. For the traffic and energy characterization, a TI evaluation board is used at the receiver as a sniffer to

overhear packet transmissions from the transmitter and record their timings accurately.

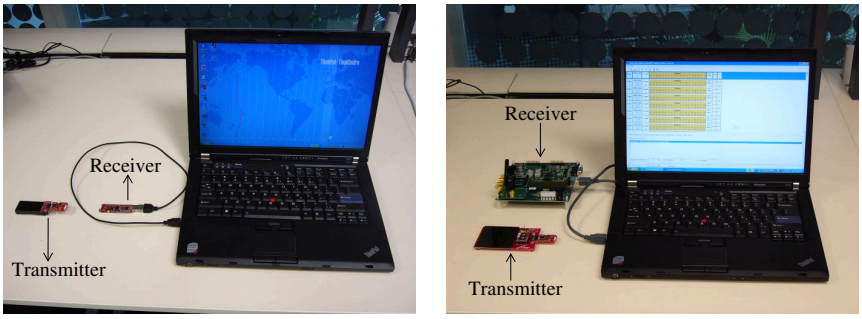

(a) Setup for link measurements (b) Setup for energy measurements

Figure 7: Experimental setup

3.2.1. Radio Characterization

To quantify the maximum transmission range, we transmit 1000 packets in an open field using the experimental setup shown in Fig. 8a, and measure the ratio of successful receptions (packet delivery ratio or PDR) at different transmitter-receiver distances. Each packet consists of 40 bytes of data (the current maximum value allowed due to software issues) with an additional 11 bytes of headers. The results are shown in Fig. 8b.

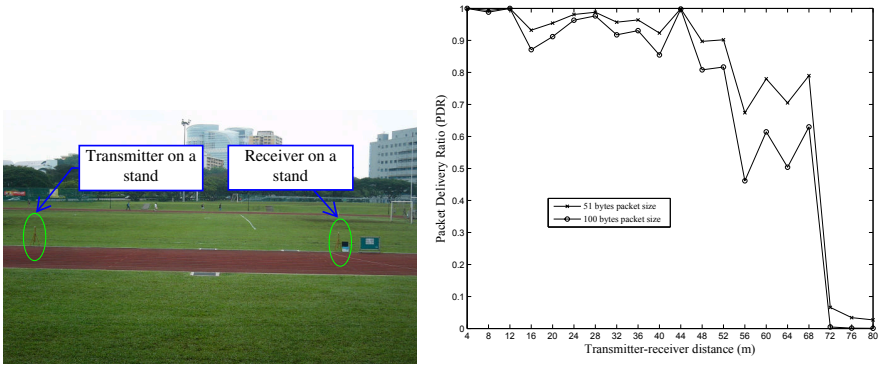

(a) Deployment (b) Results

Figure 8: Radio characterization in open field

Using the PDR values, we can compute the bit error rate (BER) at different transmitter-receiver distances and therefore we can obtain the PDR for different packet sizes. For example, the PDR results for 100 bytes packets are shown in the same graph. Although the observed PDR at shorter transmitter-receiver distances is sometimes lower than that at longer distances, the general trend is that the PDR (link quality) degrades gradually with distance, but falls sharply beyond 70m.

3.2.2. Traffic and Energy Characterization

When the transmitter is powered by the solar or thermal energy harvester, its stored energy is low initially. After some energy harvesting (charging) time, when enough energy has been harvested and accumulated in the energy storage device, the power supply for the microcontroller and transceiver will be switched on. Then, the transmitter will continuously broadcast data packets until the energy is depleted after which the microcontroller and transceiver will be turned off. The energy storage device will start to accumulate energy again and the process is repeated in the next cycle.

We characterize the traffic and energy model of each harvesting device by deploying the setup in various scenarios and recording the charging time as well as the number of packets transmitted in each cycle. Some of the scenarios that we use are shown in Table 1.

Table 1: Scenarios for characterization of traffic and energy model

Scenario No	Type of Energy Harvester	Location
1	Outdoor Solar	Outdoors, 11am
2	Indoor Solar	Directly under a fluorescent lamp (Fig. 9a)
3	Thermal	Mounted on a CPU heat sink inside a computer (Fig. 9b)

Fig. 10 illustrate the probability density functions (pdf) of the charging

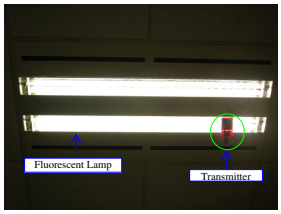

(a) Solar Energy Harvester under a fluorescent lamp

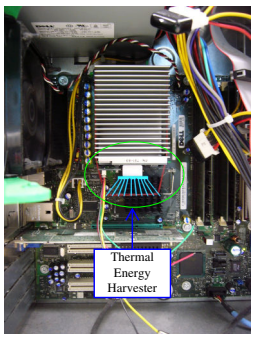

(b) Thermal Energy Harvester mounted on a CPU Heat Sink

Figure 9: Placement of energy harvesters for energy measurements

times under different scenarios obtained from 1000 charge cycles. The number of transmitted packets per cycle ranges from 17 to 19 packets with an average of 17.97 packets. A summary of the energy harvesting characteristics obtained from these experiments is given in Table 2.

Next, we investigate the temporal and spatial variation of energy harvesting, and quantify the level of time correlation in charging time across charging cycles.

- **Temporal variation:**

  For scenario 1, we plot the average energy harvesting rate obtained at 1-minute intervals for measurements collected over 30 minutes in Fig. 11. We observe that the average energy harvesting rate changes over time, decreasing (increasing) when the sky is cloudy (sunny).

- **Spatial variation:**

  For scenarios 1 and 4, we fixed the position of one node, and position the second node within a radius of 1m. For each placement, we compute the average harvesting rate over 10 minutes, and plot them in Figs. 12a and 12b for the outdoor and indoor solar energy harvesters respectively. For the outdoor scenario, the average energy harvesting rate changes for

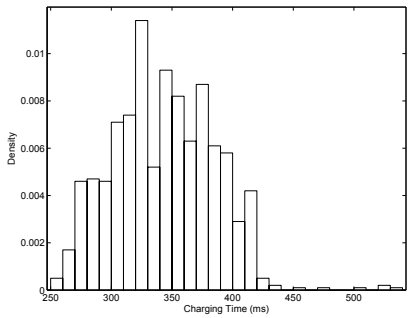

(a) Outdoor solar energy harvester at 11am

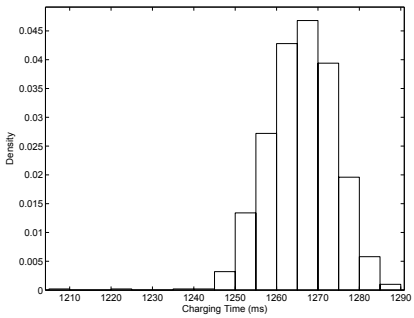

(b) Solar energy harvester directly under fluorescent lamp

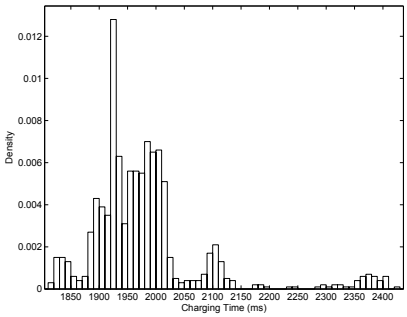

(c) Thermal energy harvester on a CPU heat sink

Figure 10: Probability density functions of charging times in different scenarios

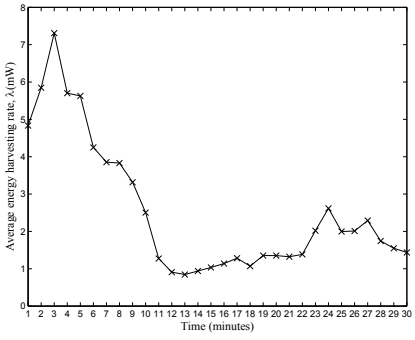

Figure 11: Average charging times of the node in different time intervals

Table 2: Charging Time Statistics for scenarios 1 to 3

	Scenario 1	Scenario 2	Scenario 3
Minimum Charging time (ms)	257.01	1208.63	1818.71
Maximum Charging time (ms)	538.32	1286.12	2422.81
Average Charging time (ms), t_c	343.31	1266.10	1980.46
Standard deviation (ms)	41.94	8.12	105.14
Bin size in Fig. 10 (ms)	10	5	10
Average time to harvest energy to send one packet (ms)	19.10	70.46	110.21
Duty cycle (%)	7.87	2.26	1.46
Average energy harvesting rate (mW)	6.59	1.89	1.22

the fixed node as the amount of cloud cover changes during our experiments while for the indoor scenario, the average energy harvesting rate for the fixed node remains constant. We observe that the average energy harvesting rates at different locations are different for both scenarios. To determine whether there is any correlation in harvesting rates between the two nodes, we use the Spearman rank correlation coefficient given by

$$r_s = 1 - \frac{6 \sum_{i=1}^{n} d_i^2}{n(n^2 - 1)} \tag{1}$$

where d_i is the difference between the ranks assigned to variables X and Y and n is the number of pairs of data. An r_s value of 1 indicate perfect correlation while an r_s value of close to zero would conclude that the variables are uncorrelated. Since there are 6 pairs of data, the critical value of r_s at 5% significance level is 0.829 obtained from statistical tables. The values of r_s for the outdoor and the indoor solar energy harvesters are 1.00 and 0.60 respectively. This means that the readings between nodes for the outdoor energy harvesters are correlated while that for indoor solar energy harvesters are not strongly correlated. This is because for

the outdoor energy harvester, the energy source is mainly from the sun while for indoor energy harvesters, there are many sources of energy from various fluorescent lamps in the room therefore readings are less likely to be correlated.

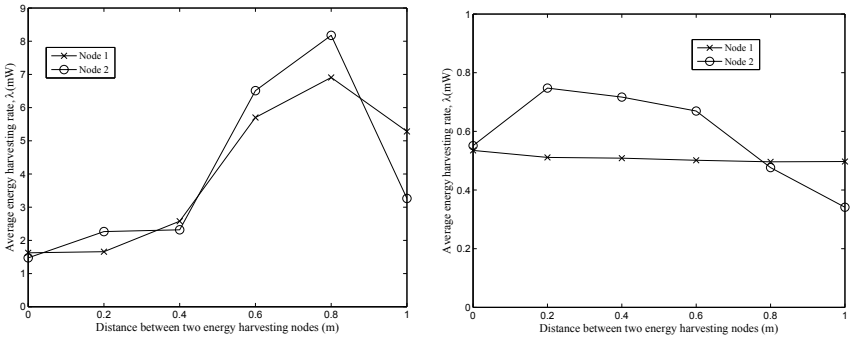

(a) Sun (b) Fluorescent lamp

Figure 12: Average charging times of nodes in the same region

- **Time correlation:**

  For each scenario, we compute the autocorrelation values for charging times recorded in different charging intervals. Fig. 13 shows the results for the different scenarios. The autocorrelation values lie between -1 and 1 with 0 indicating no correlation, 1 indicating perfect correlation and -1 indicating perfect anti-correlation. The four horizontal lines indicate 95% and 99% confidence intervals for the correlation tests. From the graph, we observe that the charging time in different intervals are uncorrelated, weakly correlated or strongly correlated depending on the type and location of the energy harvester.

From the experimental results, we can conclude the energy harvesting rate of each node (i) depends on the energy harvester used (indoor solar, outdoor solar or thermal), the location of the energy harvester as well as the time of the day (for outdoor solar cells); (ii) is uncorrelated, weakly or strongly correlated across charging cycles.

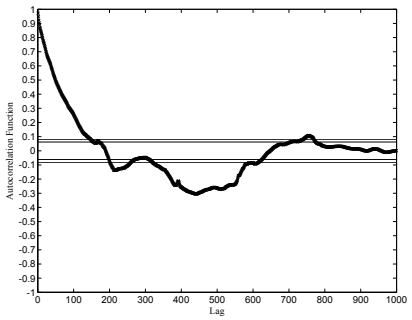

(a) Outdoor solar energy harvester at 11am

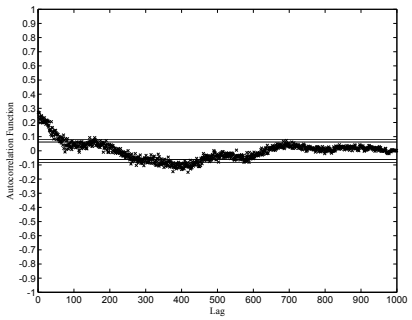

(b) Solar energy harvester under fluorescent lamp

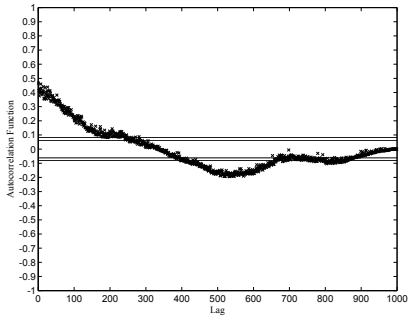

(c) Thermal energy harvester on a CPU heat sink

Figure 13: Autocorrelation function of charging times in different scenarios

3.3. Node classification

We consider both event-driven and active monitoring sensor network applications. In event-driven WSNs, data is only sent to the sink when an event is triggered by the sensed data. For example, in a target tracking WSN, data is only sent to the sink once a sensor has detected the target. Once the target has moved out of the coverage of the sensor node, data transmission will cease. In active monitoring WSNs, sensed data is periodically sent to the sink for analysis. For example, in structural health monitoring, the stability of structures need to be monitored and analyzed continuously. For event-driven WSNs, there is only one data source and the rest of the sensor nodes are relay nodes. For active monitoring WSNs, all the sensor nodes are source nodes. In addition, we also consider hybrid scenarios where some of the sensor nodes are source nodes while others are relay nodes.

Unlike traditional wireless sensor networks where the user can specify a sending rate, in WSN-HEAP the sending rate is determined by the energy harvesting rate since the source sensor node is also powered using an energy harvester. When a WSN-HEAP source node has accumulated enough energy, it will attempt to send its own sensed data if it has no packets to relay for other nodes.

Accordingly, we define three different types of nodes: *relay*, *source* and *sink* nodes.

- **Relay Node**: Relay nodes are used to forward data packets from the source nodes to the sink when they are not within direct communication range of each other. When the relay node receives any data packet in the receive state, it would buffer the data packet and schedule it for possible transmission. There are 3 states in which the relay node can be in: charging, receive and transmit states. An initially uncharged relay node will enter the charging state, where the energy consumption is minimal as most of the components of the node are shut down. It will transit into the receive state when the node is fully charged to a certain amount of

energy, E_f. If a node has a packet to transmit, it will only transit into the transmit state after it senses that the channel is clear so as to reduce the number of collisions. Otherwise, it will go into the charging state when its energy is depleted until it is fully charged to E_f and the whole cycle repeats itself. Therefore, each charging cycle consists of a charging phase, a receive phase and an optional transmit phase. The energy model and state transition diagram are illustrated in Figs. 14a and 14b respectively. Based on our empirical results from our energy harvesting characterization tests, we model the charging time in each cycle using a continuous random variable.

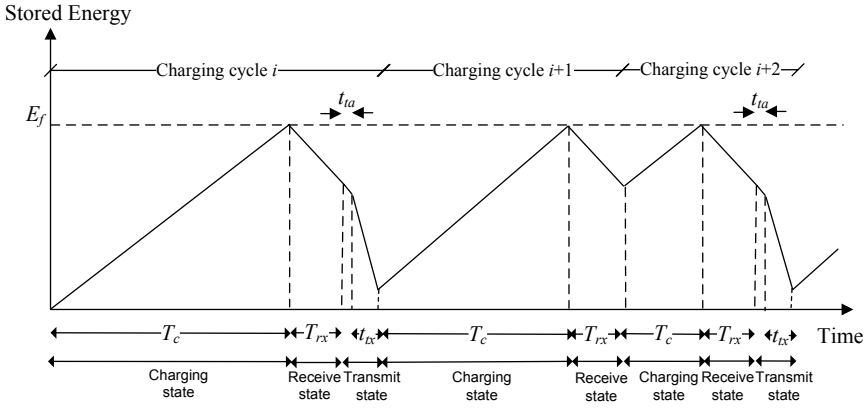

(a) Energy Model

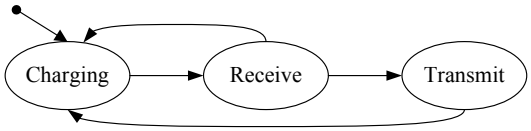

(b) State Transition Diagram

Figure 14: Characteristics of a WSN-HEAP node

- **Source Node**: The operations of the source node are similar to that of the relay node except that if it does not have to forward any received packet at the end of the receive period, it will send its own data packet in the transmit period. This means that relay packets are given higher priority than source packets. For every new data packet sent by the source node,

it would be given a unique ID. This means that every data packet can be uniquely identified using the tuple (node ID, packet ID). In addition to these two fields, each data packet will consist of the sensor data, location information and the physical layer headers.

- **Sink**: The sink is a data collection point which is connected to power mains, and therefore does not need to be charged. This means that the sink can hear data packets from its neighboring nodes continuously.

3.4. Deployment Topology

We deploy n WSN-HEAP source/relay nodes and a sink node uniformly over an interval x in the following scenarios: (i) *single-source*, comprising one source node and n-1 relay nodes (Fig. 15a), and (ii) *multi-source*, where n_s nodes ($n_s \leq n$) are randomly selected (Fig. 15b) to be source nodes. In addition, to determine the impact of node placement on network performance, we also deploy nodes randomly for the multi-source scenario as shown in Fig. 15c. We let the transmission range of the node be d which is defined as the maximum distance where the packet delivery ratio (PDR) is above the threshold Th.

Since we have deployed the sensor nodes manually, the location information of each node can be pre-programmed into the nodes in advance.

4. Energy Harvesting Opportunistic Routing Protocol (EHOR)

In this section, we present the design of our *E*nergy *H*arvesting *O*pportunistic *R*outing (EHOR) protocol which is an opportunistic routing protocol designed for WSN-HEAP. The notations used in the description of EHOR are summarized in Table 3.

4.1. Challenges of Opportunistic Routing in WSN-HEAP

Traditional OR schemes like ExOR [21] and MORE [22] are designed for nodes which are powered by either batteries or power mains. Therefore, ExOR or MORE are optimized for nodes which are always in either the transmit or

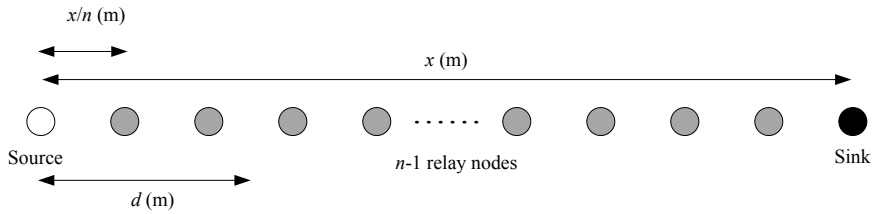

(a) Single-source uniform node placement

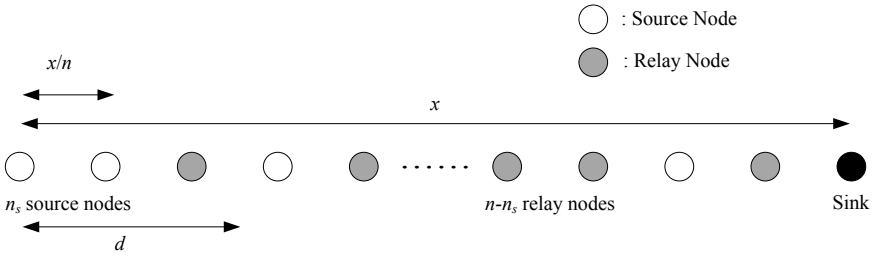

(b) Multi-source uniform node placement

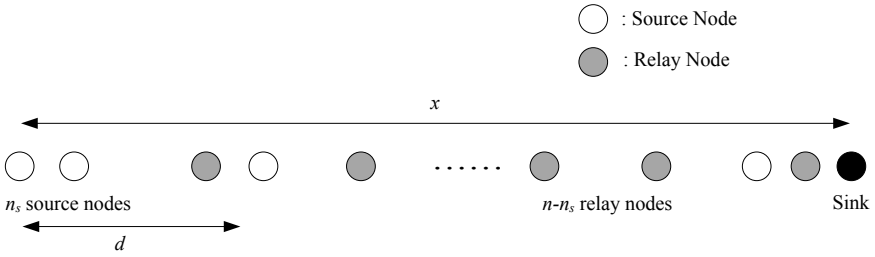

(c) Multi-source random node placement

Figure 15: Node Placement in WSN-HEAP

Table 3: Notations used in the paper

Symbol	Denotes
d	Maximum transmission range of the sensor node where packet delivery ratio is above Th
d_{sender}	Distance from the sender to the node
E_{rx}	Maximum energy required in the receive state
E_{ta}	Energy required to change state (from receive to transmit)
E_{tx}	Energy required to send a data packet
E_f	Energy of a fully charged sensor node
k	Number of regions in EHOR
n	Number of sensor nodes in the network
n_s	Number of source nodes
p	Probability that a node receives a packet
P_{rx}	Power needed when the sensor is in receive state
P_{tx}	Power needed when the sensor is in transmit state
s_{ack}	Size of an acknowledgment packet in WSF scheme
s_d	Size of a data packet
t_f	Average time taken to charge up the sensor if the initial energy of the sensor is 0
t_{prop}	Maximum propagation delay
t_{rmax}	Maximum time in the receive state
t_{ta}	Hardware turnaround time from receive to transmit state
t_{tx}	Time to send a data packet
Th	Packet data delivery threshold for determining the transmission range
x	Length of deployment area
α	Transmission rate of the sensor
β	Weightage factor in determining the priority list in EHOR
λ	Average energy harvesting rate

receive state. However, in WSN-HEAP, the nodes may be in the charging state most of the time if the energy harvesting rate is low compared to the rate of energy consumption. Therefore, the goodput of OR schemes in WSN-HEAP would be low and the delay would be high if each individual WSN-HEAP node is assigned an unique time slot for transmission. Furthermore, due to the energy characteristics of WSN-HEAP nodes, it is difficult to coordinate the nodes using traditional OR schemes since it is not possible to know which state (e.g. charging, receive) a node is in without using beacon messages. This is because each node would have different wakeup schedules as the time taken to harvest energy is different for each node as shown in our experimental results.

In ExOR, giving nodes that are closer to the destination higher relay priority will maximize the expected packet advancement. However, this method does not take into consideration the amount of energy left in the WSN-HEAP node, and hence will result in reduced network performance.

These shortcomings of traditional OR approaches motivate the design of EHOR, which uses a region-based approach by grouping nodes together to reduce delay and increase goodput. EHOR also takes into consideration the amount of energy left in the WSN-HEAP nodes as well as the expected packet advancement in the relay priority assignment so as to maximize performance.

4.2. Design Principles for EHOR

There are four desired properties of EHOR.

- **Maximize Goodput**: We need to maximize data goodput given the energy harvesting rates. This means that goodput should increase with an increase in (i) the number of WSN-HEAP nodes or (ii) the average energy harvesting rate (by using better energy harvesters).

- **Maximize Data Delivery Ratio**: We want to maximize data delivery ratio by minimizing the number of lost packets.

- **Maximize Efficiency**: We want to minimize the number of duplicate packets because they are of no value to the sink.

- **Maximize Fairness**: While goodput or data delivery ratio are important in the evaluation of any routing protocol, another important metric in sensor networks is fairness as data from every sensor node is equally important for active monitoring WSNs. If any of the sensor nodes has unequal amount of bandwidth allocation, this would have an adverse impact on the performance of the monitoring application since signals from some sensor nodes are not sent to the sink in sufficient quantity to be analyzed. To determine the fairness of various routing protocols in this paper, we use Jain's fairness metric [26] which is defined as

$$F = \frac{(\sum_{i=1}^{n_s} G_i)^2}{n_s(\sum_{i=1}^{n_s} G_i^2)}. \quad (2)$$

  where G_i is the goodput of the i^{th} sensor node. F is bounded between 0 and 1. If the sink receives the same amount of data from all the sensor nodes, F is 1. If the sink receives data from only one node, then $F \to 0$ as $n \to \infty$. The fairness metric is only computed for multi-source scenarios.

Some of these goals may be conflicting. For example, data delivery ratio can be increased by sending duplicate packets but this conflicts with our goal of maximizing efficiency which aims to minimize the number of duplicate packets. The main goal of EHOR is to achieve high goodput. Other secondary performance metrics, such as data delivery ratio, efficiency and fairness, are to illustrate the tradeoffs between different routing protocols in WSN-HEAP as well as the choice of different parameter values on the performance of EHOR.

4.3. Regioning in EHOR

The first issue in EHOR is to determine the best forwarding candidates to forward the data packets while minimizing coordination overheads and duplicate transmissions. Since we cannot determine the exact identities of nodes that are awake at any time, EHOR divides the possible set of forwarding neighbors into several regions.

A node is in the forwarding region of a sender if it is nearer to the sink than the sender is. The sender is either a source node transmitting its own

data packet or a relay node forwarding data packets from other source nodes. Upon receiving a packet, if the receiving node finds that it is not within the forwarding region of the sender, the packet will not be forwarded. Otherwise, the node will next compute the region ID which will determine its transmission priority. We let the distance from the sender to the node be d_{sender} and the number of regions be k. The region ID j can be computed using

$$j = \begin{cases} 1, & d_{sender} > d; \\ 1 + \lceil \frac{d - d_{sender}}{d} * (k-1) \rceil, & d_{sender} \leq d, \end{cases} \tag{3}$$

A region will have a lower region ID if it is closer to the sink as compared to another region that is further away from the sink. Nodes outside the transmission range of the sender may still be able to receive the data packets correctly but with very low PDR. If the sink is outside the transmission range of the sender, region 1 would consist of all the nodes outside the transmission range. Nodes with a lower region ID have higher priority to forward the data packet than nodes with a higher region ID. The region concept is illustrated in Fig. 16.

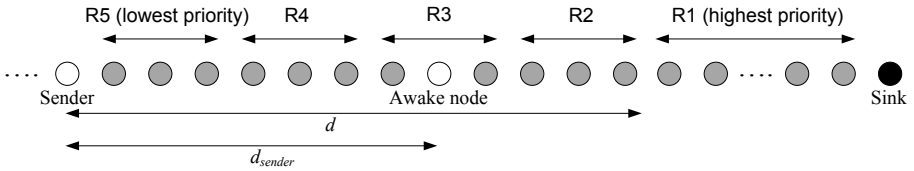

Figure 16: Illustration of region concept (k=5) with one awake node in R3

Once a packet has been received by the awake nodes in the forwarding region, EHOR has to determine which node to transmit first so as to minimize the number of collisions. Since there are k regions, we assign k time slots for the nodes to transmit. A node in the j^{th} region will transmit in the j^{th} time slot after arrival of the packet as long as the node has enough energy.

We let the size of a data transmission (including all headers) be s_d bits and the transmission rate of the sensor node be α bps. The time taken to transmit one data packet is

$$t_{tx} = s_d/\alpha. \tag{4}$$

The hardware turnaround time, which is the time for the sensor node to change from receive state to transmit state, is denoted by t_{ta}. This turnaround time is hardware-dependent. The duration of each time slot can be computed using

$$t_{slot} = t_{prop} + t_{ta} + t_{tx} \tag{5}$$

where t_{prop} is the maximum propagation delay.

The maximum time in receive state, denoted by t_{rmax}, must be greater than the number of time slots. Therefore, t_{rmax} must be more than kt_{slot}. In this paper, we let

$$t_{rmax} = (k+1)t_{slot}. \tag{6}$$

The number of regions (k) will depend on the average energy harvesting rate as well as the number of possible forwarding candidates. Since there are n sensor nodes, the number of nodes within transmission range is

$$n_1 = \lfloor \frac{d}{x} n \rfloor. \tag{7}$$

The exact value of d can be determined from actual experimentation or calculated using the propagation model of the environment in which the sensor network is being deployed in. To reduce the probability of concurrent transmissions which will lead to a wasted collision, we want an average of one awake node in each region. If the sink is outside the transmission range of the sender, there would be an additional region which consists of nodes outside the transmission range of the sender. If we let p be the probability that a node can receive a data packet from a sender, then the value of k is

$$k = \lceil n_1 p \rceil + 1. \tag{8}$$

To determine p, we need to compute the timings of various states. We let T_c and T_{rx} be random variables denoting the time in the charging and receive states in each charging cycle respectively. A data packet can only be successfully received by a node if the entire data packet is transmitted while a node is in the receive state. If we assume saturated traffic where a node will either relay

a data packet from one of the source nodes or transmit its own data packet in each charging cycle,

$$p = \frac{E[T_{rx}] - t_{tx}}{E[T_c] + E[T_{rx}] + t_{ta} + t_{tx}}. \tag{9}$$

Next, we need to determine $E[T_{rx}]$ and $E[T_c]$. The value of $E[T_{rx}]$ is dependent on the amount of traffic and the energy harvesting rate. The minimum time in the receive state for a WSN-HEAP node is t_{tx}, which is the time taken to transmit one data packet from a sender. This occurs when (i) the node receives a data packet immediately after it transits into the receive state from the charging state and (ii) the node is in region 1 of the sender and transmits immediately upon receiving the data packet. The maximum time in the receive state is t_{rmax}. Therefore, we can approximate $E[T_{rx}]$ using

$$E[T_{rx}] = \frac{t_{tx} + t_{rmax}}{2}. \tag{10}$$

We denote the maximum energy required in the receive state by E_{rx}, the energy required to transmit a data packet by E_{tx}, the energy required to change from receive state to transmit state by E_{ta} and the energy of a fully charged node by E_f. We let the receive and transmit power of the sensor be P_{rx} and P_{tx} respectively. Therefore, we have

$$E_{rx} = P_{rx}t_{rmax}, E_{tx} = P_{tx}t_{tx}, E_{ta} = \frac{P_{rx} + P_{tx}}{2}t_{ta},$$

and

$$E_f = E_{rx} + E_{ta} + E_{tx}. \tag{11}$$

Since energy is also harvested in the receive and transmit state, the average charging time is

$$E[T_c] = \frac{E_f}{\lambda} - E[T_{rx}] - t_{ta} - t_{tx} \tag{12}$$

where λ is the average energy harvesting rate. By rearranging the equations, the value of k can be calculated by solving

$$k - n\frac{d}{x} \times \frac{\lambda}{2[P_{rx}(k+1)t_{slot} + \frac{P_{rx}+P_{tx}}{2}t_{ta} + P_{tx}t_{tx}]}(kt_{slot} + t_{prop} + t_{ta}) - 1 = 0 \tag{13}$$

To illustrate EHOR, let us consider a scenario where a node receives a data packet from a sender at the time illustrated in Fig. 17. In this scenario, the node can only wait for 3 time slots before it has to transmit a data packet or shut down to recharge. If it is in region R4, it has to drop the data packet since it has insufficient energy to wait for the 4^{th} time slot to transmit. If it is in R1, it will transmit the data packet immediately upon receiving the data packet. If it is in R3, it will wait for 2 time slots in order to overhear whether other nodes in R1 and R2 have relayed the data packet. If it overhears that the data packet has already made progress towards the sink, the node will not relay the data packet.

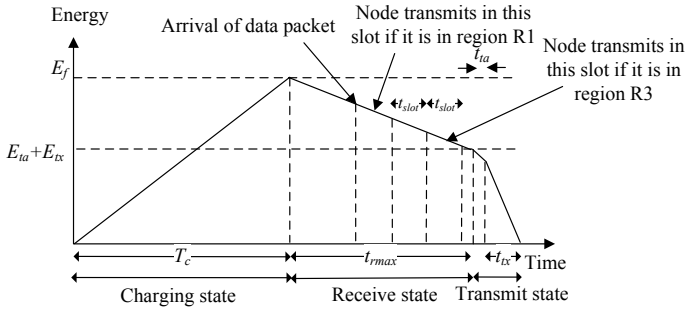

Figure 17: Example in EHOR

In EHOR, each node may receive more than one data packet in the receive state but each node can only transmit one data packet in each charging cycle. Although some received packets are being dropped if they cannot be transmitted, nodes in other regions will retransmit the data packet so the impact on data delivery ratio is not adversely affected.

4.4. Energy Considerations in EHOR

By applying regioning, nodes further away from the sender are favored without taking into consideration the energy left in a WSN-HEAP node. This results in suboptimal performance because a node that is scheduled to transmit in a particular slot may be unable to transmit although it has received the data packet. For example, in the scenario as shown in Fig. 16, nodes in R1 have

the lowest probability of receiving the data packet since they are furthest away from the sender but they have the highest probability of forwarding the data packet since they can transmit immediately after receiving the data packet if the channel is clear. Nodes in R5 have the highest probability of receiving the data packet since they are nearest the sender but they have the lowest probability of sending the data packet since they have to wait for 4 time slots to determine whether nodes in R1, R2, R3 and R4 have relayed the packet or not. At the end of this waiting time, the node may not have enough energy to wait for its transmission time slot and therefore it cannot forward the data packet.

This observation means that the performance of EHOR can be improved by devising a scheme to adjust the transmission priority based on the amount of energy left in the node, in addition to its distance from the sender. Nodes that are further away from the sender but have more remaining energy would have their priority reduced. Nodes that are nearer the sender but have less remaining energy would have their priority increased. Accordingly, if the remaining energy of the node at the end of the packet reception from the sender is E_{re}, then the j^{th} time slot in which it is scheduled to transmit in is

$$j = \lceil \beta * j_d + (1 - \beta) * j_e \rceil \tag{14}$$

where

$$j_d = \begin{cases} 1, & d_{sender} > d; \\ 1 + \frac{d - d_{sender}}{d} * (k - 1), & d_{sender} \leq d, \end{cases}$$

and

$$j_e = \begin{cases} 1, & d_{sender} > d; \\ \frac{E_{re} - E_{ta} - E_{tx}}{t_{slot} P_{rx}}, & d_{sender} \leq d. \end{cases}$$

The factor, β, $0 \leq \beta \leq 1$, weighs the forwarding priority of a node between its residual energy and quality of the direct link (based on distance) with the sink. With $\beta = 0$ (1), nodes with lower remaining energy (nearer the sink) will be assigned higher forwarding priority.

The detailed algorithms of EHOR are illustrated in Figs. 18 to 21.

EHOR:

Step 1. Compute E_f using (11)

Step 2. Compute k using (13)

Step 3. Stay in the charging state until the accumulated energy reaches E_f

Step 4. Go to receive state

while Node is in receive state **do**

  if Node receives a data packet **then**

    ReceiveDataPacket

  end if

  if Any data packet is due for transmission **then**

    TransmitDataPacket

  end if

  if Time in receive state = t_{rmax} **then**

    EndReceiveState

  end if

end while

Go to Step 3.

Figure 18: Main EHOR algorithm

procedure ReceiveDataPacket

Check for duplicate packet in the buffer

if Packet is already in buffer **then**

Drop received data packet

if Sender is nearer to the sink than the node is **then**

Remove data packet from the buffer as the packet has already made progress towards the sink

end if

else ▷ packet is not in buffer

if Sender is nearer to the sink than the node is **then**

Drop received data packet

else

Store data packet in buffer and schedule the packet to transmit in the time slot computed by (14)

end if

end if

end procedure

Figure 19: Algorithm when a node receives a data packet in the receive state

```
procedure TransmitDataPacket
    Remove data packet, which is scheduled to transmit now, from the buffer
    if Channel is clear then
        Drop all existing data packets in the buffer
        Transmit data packet
        Go to charging state
    else
        Drop data packet
        Remain in receive state
    end if
end procedure
```

Figure 20: Algorithm when any data packet is due for transmission

```
procedure EndReceiveState
    Drop all data packets in the buffer
    if Node is a source node then
        if Channel is clear then
            Transmit own data packet
        else
            Go to charging state
        end if
    else                                          ▷ Node is a relay node
        Go to charging state
    end if
end procedure
```

Figure 21: Algorithm when maximum receive time is reached

5. Performance Analysis

We use the Qualnet network simulator [27] to assess the performance of EHOR. We modify Qualnet to incorporate the energy model as shown in Fig. 14a. The main performance metric is *goodput* while other performance metrics of interest include source sending rate, throughput, data delivery ratio, efficiency, hop count and fairness. Each data point is derived from the average of 10 simulation runs of duration 200s each using different seeds. Each data packet is 100 bytes while the acknowledgment packet in the WSF scheme is 15 bytes.

We have incorporated the specifications of the TI energy harvesting sensor node [5] into our simulations. The current draw for the RF transceiver is 24.2 mA and 27.9 mA for receiving and transmitting (at 1dBm) respectively as measured in [28]. The output voltage by the energy harvesting node is 3 V. Accordingly, the power consumption for reception and transmission are $P_{rx} =$ 72.6 mW and $P_{tx} = 83.7$ mW respectively. For a packet size, s_d, of 51 bytes used in our energy characterization tests, and data rate, $\alpha = 250$ kbps, the packet transmission time, $t_{tx} = 1.632$ ms. The total energy consumed during node operation, E_{total}, is given by:

$$E_{total} = n_{pkt} P_{tx} t_{tx},$$

where n_{pkt} is the average number of packets transmitted per charging cycle. Using the average charging time, t_c, obtained from Table 2, $\lambda = \frac{E_{total}}{t_c + n_{pkt} t_{tx}}$ can be computed for each scenario, and is tabulated in Table 2.

The transmission rate of the node is 250kbps while the hardware turnaround time is 0.192 ms. We fixed x at 300m and Th at 10%. Using the radio characterization results in Section 3.2.1, the transmission range used in the computation of the number of regions in EHOR, d, is 70m. We model the radio propagation model using a lognormal shadowing model and a Ricean fading model which approximates closely the empirical results of the radio characterization tests. For traditional routing protocols, strong links are preferred over weak links, therefore Th is usually set to a high value (e.g. 90%). However in opportunistic

routing, we would want to make use of weak but long-distance links. Therefore, Th is set to a lower threshold to increase the transmission range. These parameter values are shown in Table 4.

Table 4: Values of Various Variables used in Performance Analysis

Parameter	Value
d	70m
n	20 to 300
P_{rx}	72.6 mW
P_{tx}	83.7 mW
s_{ack}	15 bytes
s_d	100 bytes
t_{ta}	0.192 ms
Th	0.1
x	300m
α	250 kbps
β	0.0, 0.2, 0.4, 0.6, 0.8, 1.0
Shadowing Model	Lognormal
Fading Model	Ricean
Simulation Time	200 seconds

The performance metrics which we considered and their definitions are summarized in Table 5.

5.1. Characterization of EHOR

First, we need to analyze the behavior of EHOR under different scenarios using a uniformly distributed topology as illustrated in Figs. 15a and 15b.

5.1.1. Impact of β in single-source scenario

The value of β is a key design parameter in EHOR, therefore we need to determine the impact of different values of β on network performance. We

Table 5: Performance Metrics

Parameter	Value
Source Sending Rate (SR)	Combined rate of data packets sent by all the source nodes
Throughput (T)	Rate of data packets (including duplicate packets) received by the sink
Goodput (G)	Rate of unique data packets received by the sink
Data Delivery Ratio (DR)	Ratio of G to SR
Efficiency (η)	Ratio of G to T
Hop Count (H)	Average number of times a packet is transmitted until it reaches the sink
Fairness (F)	Computed using (2)

consider a single-source scenario with λ=10mW and vary the number of relay nodes from 20 to 300. The performance results are illustrated in Fig. 22 for different values of β from 0 to 1.

First, we consider the source sending rate (SR) which is the combined rate of packets sent by all the sources. The source sending rate varies because the source node will only transmit at the end of a receive period after it senses that the channel is clear so as to minimize collisions. Furthermore, since the number of regions (k) increases as the number of relay nodes increases, t_{rmax} will also increase, resulting in lower sending rate from each source. From the graphs, the choice of β has little influence on SR.

Next, we consider throughput (T) of the network. The throughput of the network is defined as the rate of data packets, including duplicate packets, received by the sink. From the results, it is clear that setting β to 0 gives the highest throughput. However, the throughput metric is not a good performance metric as it includes the duplicate packets which are of no value to the sink. Therefore, we consider goodput (G) as our main performance metric which is defined as the rate of unique packets received by the sink. In the single-source

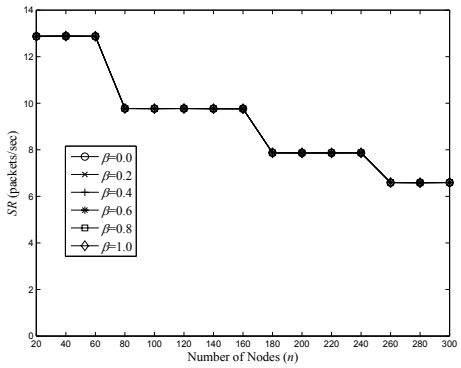

(a) Source Sending Rate

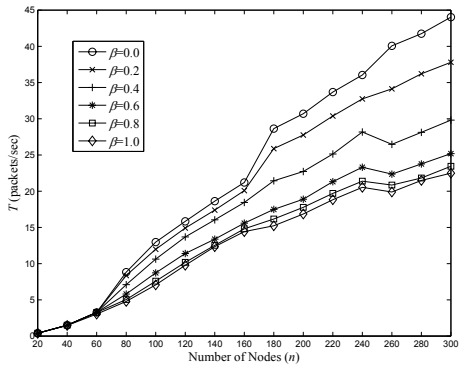

(b) Throughput

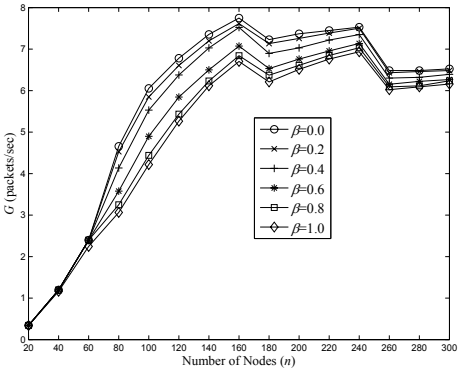

(c) Goodput

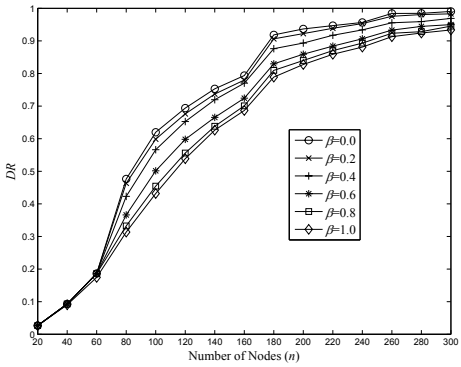

(d) Data Delivery Ratio

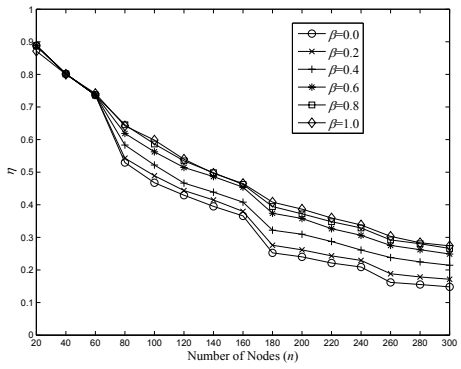

(e) Efficiency

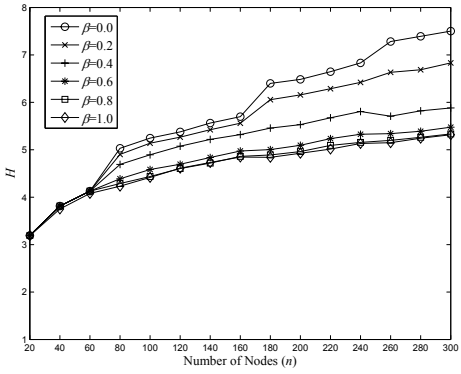

(f) Hop Count

Figure 22: Performance results for a single-source scenario with varying number of relay nodes (n=20 to 300,n_s=1,λ=10mW)

scenario, setting β to 0 gives the highest goodput. This is because by considering only energy constraints, every relay node will attempt to transmit the received data packet at the end of the receive cycle when there is little energy left, thereby increasing the probability of a successful data delivery to the sink.

The data delivery ratio (DR) is the ratio of goodput (G) to source sending rate (SR). This metric computes the probability of a packet being delivered to the sink for every packet transmitted by the source node. Similarly, DR is maximized by having β=0. We also consider efficiency and hop count. Efficiency (η) is the ratio of goodput (G) to throughput (T). It can also be described as the probability of a received packet being a unique packet when received by the sink. The metric hop count (H) is the average number of packet transmissions before the packet reaches the sink. High efficiency and low hop count are desirable in order to maximize the usage of the harvested energy. Although setting β to 0 gives the highest throughput, goodput and data delivery ratio, it performs the worst in terms of efficiency and hop count.

5.1.2. Impact of β in multi-source scenarios

We consider a multi-source scenario where the total number of sensor nodes (n) is set to 300 with the number of source nodes (n_s) varying from 20 to 300. The results are illustrated in Fig. 23. Unlike the single-source scenario, setting β to 0 no longer maximizes goodput when the number of source nodes is high even though throughput is maximized. This clearly shows that high throughput does not always equate high goodput. The data delivery ratio and hop count decreases while efficiency increases when β increases. For multi-source scenarios, we also consider fairness. For small number of source nodes, different values of β have only minimal impact on fairness but for large number of source nodes, setting β to 0 maximizes fairness due to an increase in the number of packets received from the source nodes furthest away from the sink.

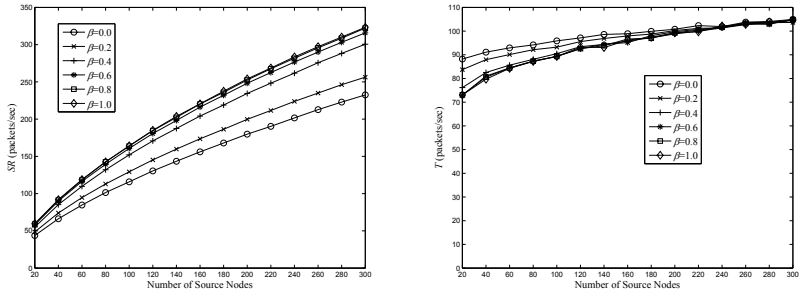

(a) Source Sending Rate

(b) Throughput

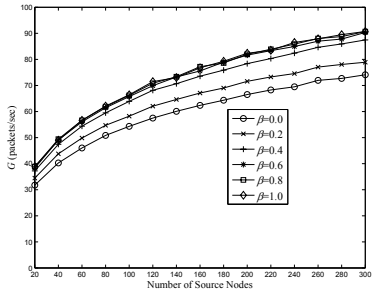

(c) Goodput

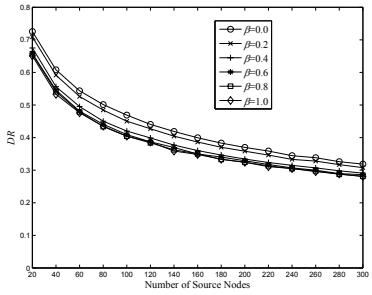

(d) Data Delivery Ratio

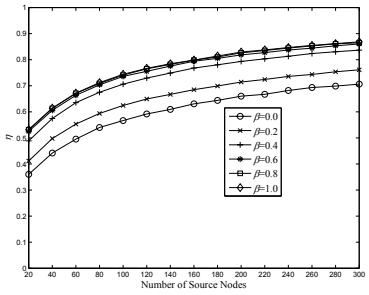

(e) Efficiency

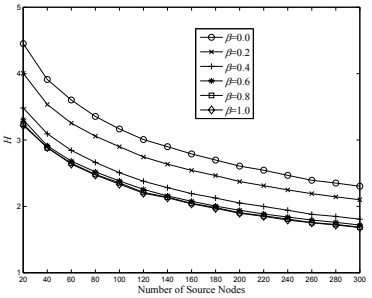

(f) Hop Count

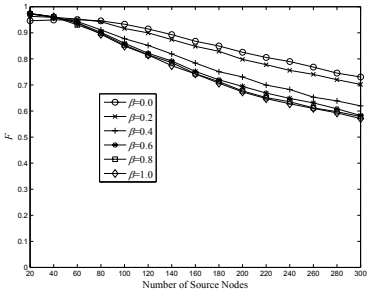

(g) Fairness

Figure 23: Performance results for a multi-source scenario with varying number of source nodes (n=300,n_s=20 to 300,λ=10mW)

5.1.3. Varying energy harvesting rates

We vary the average energy harvesting rate (λ), from 2mW to 20mW, to take into account varying energy harvesting rates when different types and sizes of energy harvesters are used. Fig. 24 illustrates the scenarios with 1, 150 and 300 source nodes with a total of 300 sensor nodes. When there is only 1 source node, setting β to 0 maximizes goodput when the energy harvesting rate is less than 14 mW. However, when there are 150 or 300 source nodes, setting β to 0 gives the worst goodput.

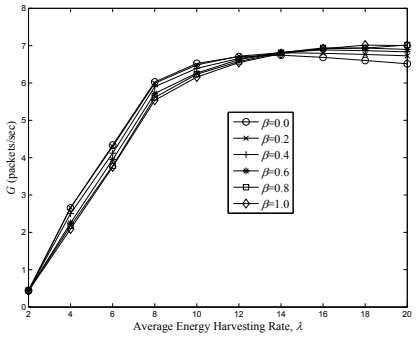

(a) Single Source (n_s=1)

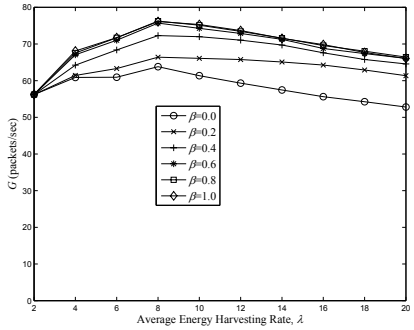

(b) 50% Source Nodes (n_s=150)

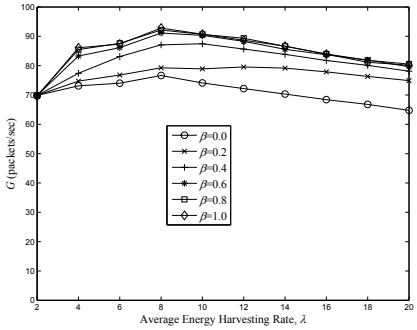

(c) 100% Source nodes (n_s=300)

Figure 24: Performance results with varying energy harvesting rates (n=300,λ=2 to 20 mW)

5.1.4. Analysis

From the results presented so far, we can infer some properties of EHOR. When there are only one source node, goodput is maximized by considering

the remaining energy alone (β=0) when assigning transmission priorities. However, this reduces efficiency as the number of transmissions required per packet will increase because EHOR has to use some short-distance links instead of long-distance ones. When the number of source nodes increases, there will be increased MAC contention due to more transmissions by the nodes. Therefore, by giving long-distance links higher priority ($\beta > 0$), goodput will improve as this means that the number of retransmissions needed per packet is reduced, thereby reducing the possibility of collisions. In general, as β increases, the average number of hops needed per packet decreases due to the usage of more long-distance links and goodput may increase due to less MAC collisions and interference. However, goodput may also decrease due to less retransmission opportunities as the node may need to drop the packet before it is due for retransmission as it uses up its harvested energy and needs to recharge. Hence, these two opposing effects result in an optimal value of β to be used when we vary the number of sources and energy harvesting rates. Furthermore, we can also observe that there is no correlation between goodput and fairness in some scenarios. For example, when we vary the number of sources in Fig. 23, setting $\beta = 0$ gives the highest fairness but the lowest goodput. This is because the increase in goodput is due to higher goodput from nodes nearer the sink, therefore decreasing the fairness since less packets are received from nodes further away from the sink. This shows the maximizing all the performance metrics is not possible in some scenarios and there are tradeoffs that need to be made.

5.2. Comparison of EHOR with other routing protocols

To determine the performance gains from using regioning as well as energy considerations in WSN-HEAP, we also consider opportunistic routing without these enhancements. This protocol is labeled as OR in Figs. 25 to 29. In OR, each possible forwarding node is given a unique timeslot to retransmit the received data packet, therefore the maximum time spent in a receive period is given by

$$t_{rmax} = (n_1 + 1)t_{slot} \tag{15}$$

where n_1 is the number of forwarding candidates which is computed using (7).

In addition, we compare EHOR with two other different routing protocols suited for WSN-HEAP using a broadcast-based geographic routing protocol (GR-DD) for WSN-HEAP [19] and an asynchronous wakeup schedule protocol (WSF) [20]. For the WSF protocol, we use two combinations using (7,3,1) and (73,9,1) block design as described in Section 2.

GR-DD differs from EHOR in three ways:

- In GR-DD, the time spent in the receive state is fixed at $2t_{tx}$ while in EHOR, the time spent in the receive state is not fixed and t_{rmax} is calculated using the total number of nodes and the average energy harvesting rate.

- GR-DD needs non-volatile memory as packets received need to be stored in the buffer for transmission in future charging cycles if the packet cannot be transmitted at the end of the current charging cycle. In EHOR, any packet in the buffer is dropped at the end of the charging cycle if it cannot be transmitted.

- Unlike EHOR, GR-DD is not an opportunistic routing protocol since it does not attempt to overhear whether the packet has already made progress before transmission.

WSF differs from EHOR in the following two ways:

- A successful data transmission requires the reception of 3 packets: the beacon packet, the data packet and the ACK packet. If only the first 2 packets are successfully transmitted, there would be duplicate packets since the sender has to retransmit the packet to possibly another forwarder. For EHOR, a successful data transmission requires only the reception of the data packet.

- EHOR, like other OR schemes in general, uses the broadcast nature of the wireless medium to send the packets to as many forwarding nodes as possible while WSF uses unicast routing.

For EHOR, we set β to 0.6 as this value achieves high throughput for most scenarios. First, we consider the scenario where there is one source node with varying number of relay nodes. The results are shown in Fig. 25. The results show that only EHOR scales to large number of relay nodes while the WSF scheme works well for fewer relay nodes. The WSF scheme is not scalable to large number of nodes due to excessive MAC collisions during the beaconing process. From the hop count metric, it is also clear that WSF can only make use of good-quality but short-range links, otherwise data transmission would not be successful.

Next, we consider the scenario where we vary the number of sources. The comparisons between EHOR, OR, GR-DD and WSF are illustrated in Fig. 26. EHOR achieves higher goodput and efficiency compared to the rest of the routing protocols and also requires less retransmissions by relay nodes. For the WSF protocol, the number of hops decreases with increasing number of source nodes as more packets are received from the source nodes closer the sink, thereby reducing the average number of hops required. Although OR maximizes fairness in some scenarios, the goodput is low as compared to EHOR.

Finally, we consider scenarios with varying energy harvesting rates. The results are shown in Fig. 27 for scenarios with 1, 150 and 300 source nodes. For all the scenarios, only EHOR can achieve high goodput consistently.

Next, we study the impact of node failure on network performance. There are a total of 300 nodes with 30 source nodes. We vary the number of failed relay nodes from 10% to 100% which are randomly chosen from the set of relay nodes. Fig. 28 shows that EHOR performs the best in most cases except when the failure rate is very high (i.e. more than 80% in this scenario) in which case GR-DD performs the best. The performance of EHOR degrades gracefully because EHOR uses opportunistic retransmissions, so even if some nodes failed, other nodes can retransmit the data packets. The performance of GR-DD and WSF improves when failure rate increases resulting in overall fewer sensor nodes, thereby reducing channel contention. This shows that both GR-DD and WSF are not suitable for use in dense sensor networks.

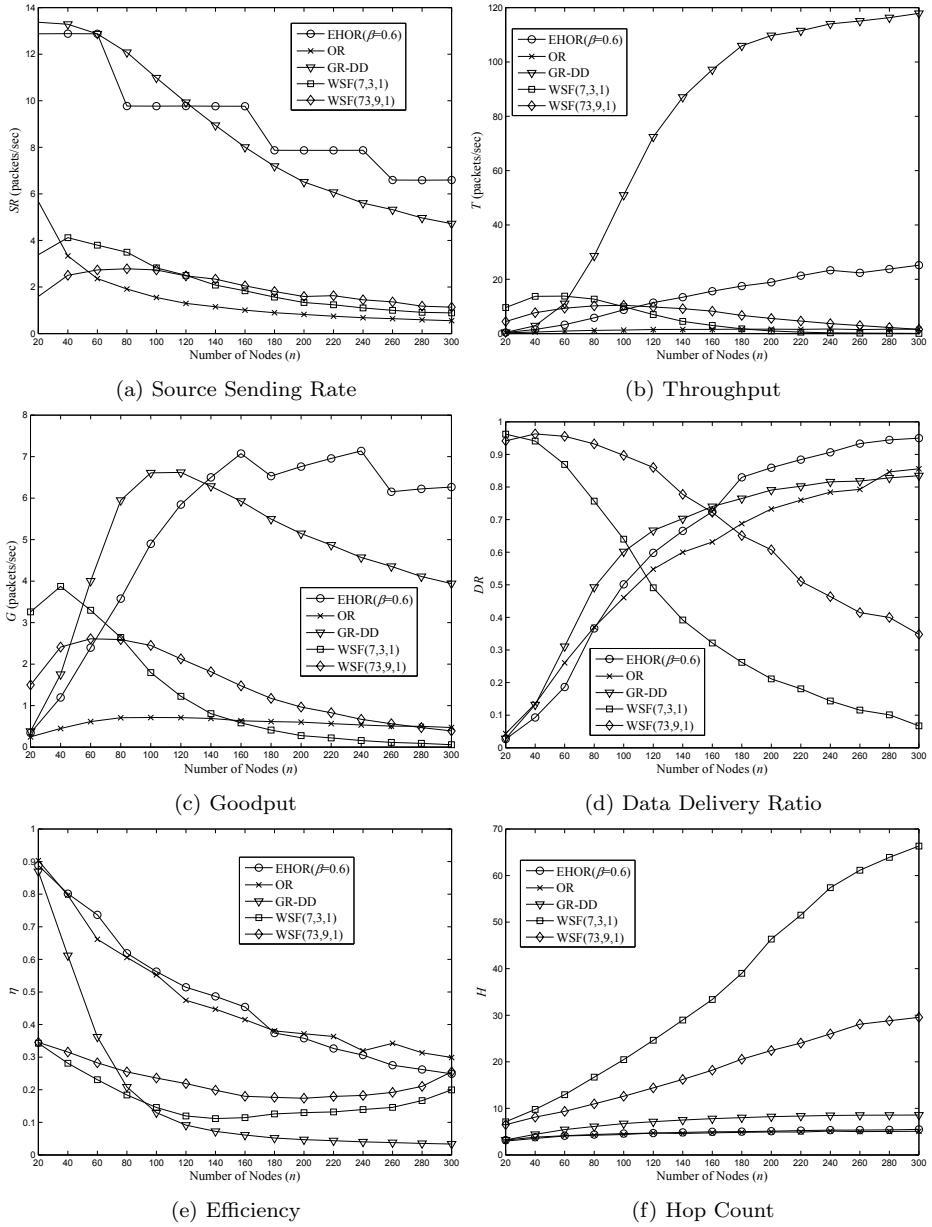

(a) Source Sending Rate

(b) Throughput

(c) Goodput

(d) Data Delivery Ratio

(e) Efficiency

(f) Hop Count

Figure 25: Performance comparison between different routing protocols for a single-source scenario with varying number of relay nodes (n=20 to 300,n_s=1,λ=10mW)

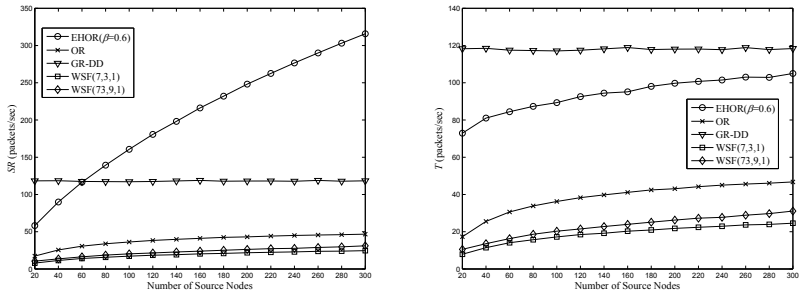

(a) Source Sending Rate

(b) Throughput

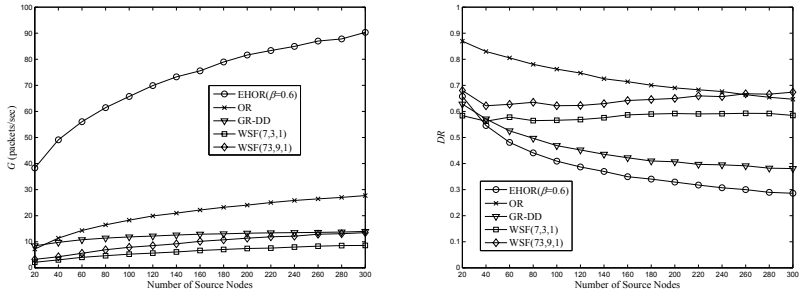

(c) Goodput

(d) Data Delivery Ratio

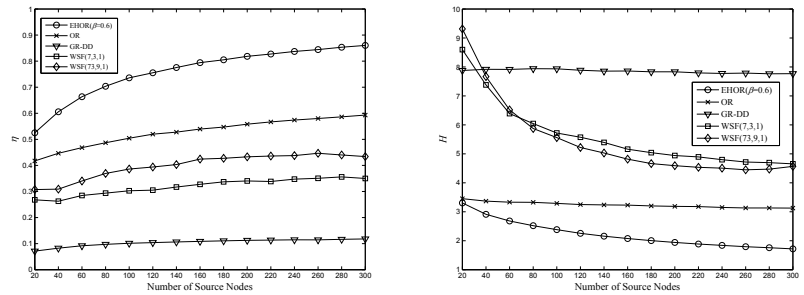

(e) Efficiency

(f) Hop Count

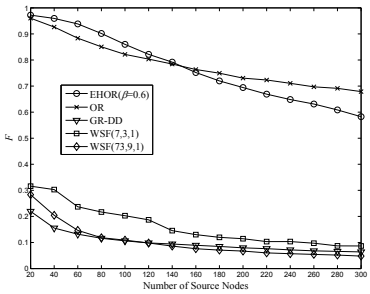

(g) Fairness

Figure 26: Performance comparison between different routing protocols with varying number of source nodes (n=300,n_s=20 to 300,λ=10mW)

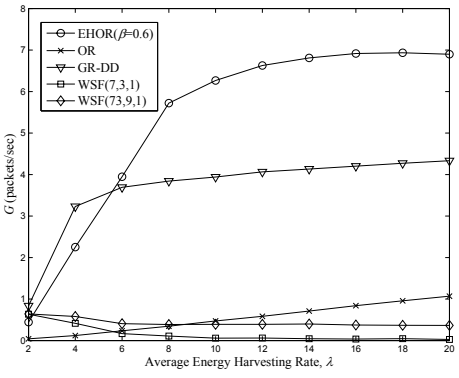

(a) Single Source (n_s=1)

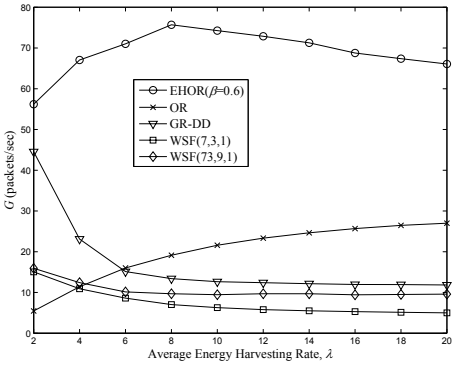

(b) 50% Source Nodes (n_s=150)

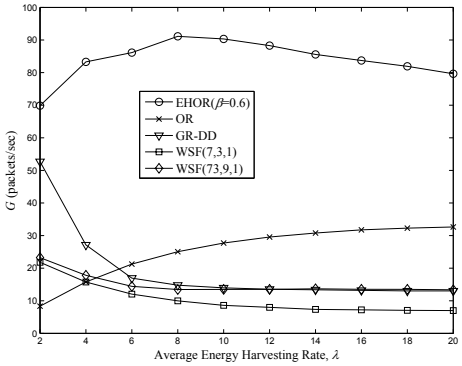

(c) 100% Source Nodes (n_s=300)

Figure 27: Performance comparison between different routing protocols with varying energy harvesting rates (n=300,λ=2 to 20 mW)

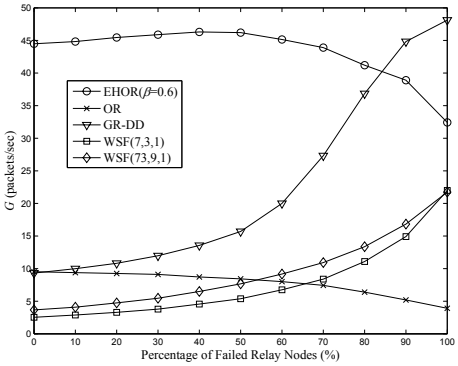

Figure 28: Goodput of different protocols in the presence of node failures (n=300,n_s=30, λ=10 mW)

Finally, we determine the impact of node placement on network performance. The nodes are placed randomly as shown in Fig. 15c and we vary the total number of nodes from 20 to 300 with a total of 20 source nodes. Fig. 29 shows that goodput may increase or decrease for low number of nodes, however at high node density, the difference is not significant for all the protocols. The results show that EHOR gives the best performance. This is because EHOR uses opportunistic retransmissions so it performs well even if the nodes are not uniformly distributed as long as there are sufficient nodes within the forwarding region of the sender.

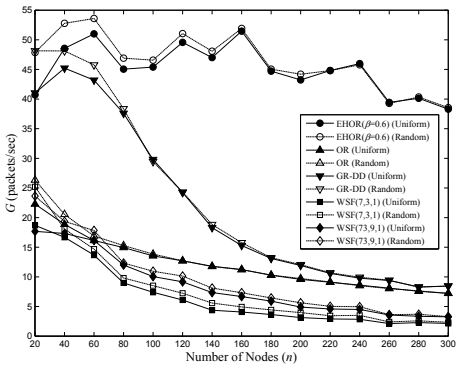

Figure 29: Goodput of different protocols when the nodes are randomly distributed (n=20 to 300,n_s=20, λ=10 mW)

From the performance analysis, we find that EHOR improves performance over opportunistic routing without regioning and residual energy considerations (OR) because

1. Regioning helps to improve performance by grouping WSN-HEAP nodes together, thereby reducing the time required in the receive state. This optimizes the use of the harvested energy so that more packets can be sent or forwarded by the nodes.
2. By considering residual energy, each WSN-HEAP node has a higher probability of forwarding the received packet, thereby increasing goodput. However, this benefit has to be carefully weighed against more transmissions

required due to the use of more short-range links.

GR-DD does not perform well compared to EHOR because

1. It does not attempt to listen to whether a packet has been successfully retransmitted before transmission, resulting in the sink receiving a lot of duplicate packets besides causing more collisions and interference.
2. The receive period is fixed in GR-DD but is variable in EHOR, thereby reducing the number of MAC collisions through using less transmissions and utilizing more long-distance links.

WSF does not perform well in WSN-HEAP as compared to EHOR because

1. The duty cycle of WSF is fixed and not adapted to the energy harvesting rate. This is because WSF is optimized for battery-operated WSNs where network lifetime is of key consideration. However, in WSN-HEAP, harvested energy could be replenished and therefore goodput is our key consideration. In EHOR, the number of regions can change when the energy harvesting rates change, thereby optimizing network performance.
2. Beaconing and acknowledgments are required for WSF in WSN-HEAP, and some bandwidth has to be allocated to these control packets, thereby reducing overall performance.
3. A successful transmission requires three successful successive transmissions, therefore it cannot make use of long-distance links. This is illustrated in the performance graphs where the average number of hops using the WSF scheme is much larger than other routing protocols.

6. Conclusion

In this paper, we have designed an opportunistic routing protocol (EHOR) for wireless sensor networks that are powered solely using energy harvesting devices. First, we use a regioning approach to group nodes together in EHOR to reduce delay and improve goodput as compared to conventional opportunistic routing protocols. Next, we further improve EHOR's performance by taking

into consideration the amount of residual energy in each node in addition to its distance from the sender when determining its transmission priority. We evaluate EHOR using extensive simulations by varying the number of nodes as well as the energy harvesting using the energy charging characteristics of commercially available energy harvesting sensor nodes. The results show that assigning transmission priorities to the nodes according to distance and residual energy is important to achieve optimal network performance. When compared to other non-OR routing protocols, EHOR achieves high goodput, efficiency, data delivery ratio and fairness. For future work, we are extending our protocol design to a 2D topology. In addition, we are exploring the use of network coding to improve performance.

References

[1] J. Yick, B. Mukherjee, D. Ghosal, Wireless sensor network survey, Computer Networks Journal 52 (12) (2008) 2292–2330.

[2] I. F. Akyildiz, T. Melodia, K. R. Chowdhury, A Survey on Wireless Multimedia Sensor Networks, Computer Networks Journal 51 (4) (2007) 921–960.

[3] G. Anastasi, M. Conti, M. D. Francesco, A. Passarella, Energy conservation in wireless sensor networks: A survey, Ad Hoc Networks Journal 7 (3) (2009) 537–568.

[4] J. A. Paradiso, T. Starner, Energy Scavenging for Mobile and Wireless Electronics, IEEE Pervasive Computing 4 (1) (2005) 18–27.

[5] MSP430 Solar Energy Harvesting Development Tool (eZ430-RF2500-SEH) from Texas Instruments.
URL `http://www.ti.com`

[6] Microstrain.
URL `http://www.microstrain.com`

[7] Ambiosystems.
URL http://www.ambiosystems.com

[8] P. Dutta, J. Hui, J. Jeong, S. Kim, C. Sharp, J. Taneja, G. Tolle, K. Whitehouse, D. Culler, Trio: Enabling Sustainable and Scalable Outdoor Wireless Sensor Network deployments, in: IPSN, 2006, pp. 407–415.

[9] P. Sikka, P. Corke, P. Valencia, C. Crossman, D. Swain, G. Bishop-Hurley, Wireless Adhoc Sensor and Actuator Networks on the Farm, in: IPSN, 2006, pp. 492–499.

[10] G. Park, C. R. Farrar, M. D. Todd, W. Hodgkiss, T. Rosing, Energy Harvesting for Structural Health Monitoring Sensor Networks, Tech. rep., Los Alamos National Laboratory (Feb. 2007).

[11] T. Voigt, H. Ritter, J. Schiller, Utilizing Solar Power in Wireless Sensor Networks, in: IEEE International Conference on Local Computer Networks (LCN), 2003, pp. 416–422.

[12] D. Noh, J. Kim, J. Lee, D. Lee, H. Kwon, H. Shin, Priority-based Routing for Solar-Powered Wireless Sensor Networks, in: ISWPC, 2007, pp. 53–58.

[13] K. Zeng, K. Ren, W. Lou, P. J. Moran, Energy aware efficient geographic routing in lossy wireless sensor networks with environmental energy supply, Wireless Networks 15 (1) (2009) 39–51.

[14] H. Kwon, D. Noh, J. Kim, J. Lee, D. Lee, H. Shin, Low-Latency Routing for Energy-Harvesting Sensor Networks, in: UIC, 2007, pp. 442–433.

[15] L. C. Klopfenstein, E. Lattanzi, A. Bogliolo, Implementing Energetically Sustainable Routing Algorithms for Autonomous WSNs, in: WoWMoM, 2007, pp. 1–6.

[16] E. Lattanzi, E. Regini, A. Acquaviva, A. Bogliolo, Energetic sustainability of routing algorithms for energy-harvesting wireless sensor networks, Computer Communications 30 (14-15) (2007) 2976–2986.

[17] L. Lin, N. B. Shroff, R. Srikant, Asymptotically Optimal Energy-Aware Routing for Multihop Wireless Networks With Renewable Energy Sources, IEEE/ACM Transactions on Networking 15 (5) (2007) 1021–1034.

[18] A. Kailas, M. A. Ingram, Y. Zhang, A Novel Routing Metric for Environmentally-Powered Sensors with Hybrid Energy Storage Systems, in: Wireless VITAE, 2009.

[19] Z. A. Eu, H.-P. Tan, W. K. G. Seah, Routing and Relay Node Placement in Wireless Sensor Networks Powered by Ambient Energy Harvesting, in: IEEE WCNC, 2009.

[20] R. Zheng, J. C. Hou, L. Sha, Asynchronous Wakeup for Ad Hoc Networks, in: MobiHoc, 2003, pp. 35–45.

[21] S. Biswas, R. Morris, ExOR: Opportunistic Multi-Hop Routing for Wireless Networks, in: ACM SIGCOMM, 2005, pp. 133–143.

[22] S. Chachulski, M. Jennings, S. Katti, D. Katabi, Trading Structure for Randomness in Wireless Opportunistic Routing, in: ACM SIGCOMM, 2007, pp. 169–180.

[23] J. Wu, M. Lu, F. Li, Utility-Based Opportunistic Routing in Multi-hop Wireless Networks, in: IEEE International Conference on Distributed Computing Systems (ICDCS), 2008, pp. 470–477.

[24] M. Zorzi, R. Rao, Geographic Random Forwarding (GeRaF) for Ad Hoc and Sensor Networks: Multihop Performance, IEEE Trans. Mobile Comput. 2 (4) (2003) 337–348.

[25] Micropelt thermogenerator.
URL `http://www.micropelt.com`

[26] R. Jain, D. M. Chiu, W. Hawe, A quantitative measure of fairness and discrimination for resource allocation in shared computer system, Tech.

Rep. DEC-TR-301, Digital Equipement Corp (Sep. 1984).
URL http://www.cs.wustl.edu/jain/papers/fairness.htm

[27] Qualnet network simulator.
URL http://www.scalable-networks.com

[28] T. Watteyne, eZWSN: Experimenting with Wireless Sensor Networks using the eZ430-RF2500 (2008).
URL http://cnx.org/content/col10684/1.10/